Printed-Circuit Antennas for Ultra-Wideband Monitoring Applications

Marjan Mokhtaari and Jens Bornemann

Department of Electrical and Computer Engineering, University of Victoria
PO Box 3055, Victoria, BC, V8W 3P6, Canada
j.bornemann@ieee.org

***Abstract* — Two new printed-circuit antennas for ultra-wideband (UWB) monitoring applications are introduced. Both microstrip and coplanar waveguide antennas operate between 3 GHz and 30 GHz with a return loss of 10 dB. The vertically polarized omnidirectional radiation characteristics in the lower frequency band change to a more directional pattern at higher frequencies. The cross-polar field component increases with frequency and gives rise to possible dual-polarized applications for the microstrip antenna. Overall, the coplanar antenna shows slightly better performance. Amplitude and group-delay responses are demonstrated over the entire 3-30 GHz band, and radiation patterns at selected frequencies are shown.**

I. Introduction

As wireless data transmission applications are increasing in number and in frequency, e.g. up to 60 GHz [1], there is an obvious need for proper monitoring equipment in order to enforce standards or investigate related topics. The range of sensor and monitoring applications is wide-spread and addresses issues such as EIRP compliance [2], immunity tests [3], interference [4], high-power microwave detection [5], health-related testing [6], [7], and many more.

Therefore, associated test equipment for sensing and monitoring are developed. Such systems must have ultra-wideband (UWB) performance in order to detect electromagnetic emissions in a wide range of frequencies. Sensor networks for wireless applications have been proposed, e.g. [8], and EMC testing equipment for mobile phones is being developed, e.g. [9]. Recently, a system for EMI measurements up to 26 GHz has been presented [10].

Within such testing systems, the UWB antenna is of special importance as it must provide the bandwidth for an often multi-band receiver system. For initial tests and certification procedures, TEM horns can be used in chamber measurement setups, e.g. [11]. For mobile monitoring, however, printed-circuit antennas are more appropriate, and a large number of printed-circuit antennas have been developed within the last several years, e.g. [12], [13].

However, many designs are confined to the 3-10 GHz range for compliance with the FCC approved bandwidth. Only rarely and more recently have monopole-type antennas been presented that extend the applicable frequency range to 20 GHz [14], 30 GHz [15], 40 GHz [16], 50 GHz [17] and even 60 GHz [18]. Common to most of these applications is a printed-circuit monopole whose return loss has been optimized to cover a much larger band that the originally 3-10 GHz range, but whose change in pattern characteristics over the wider band has been accepted as unavoidable.

This paper presents two new designs, one in microstrip and one in coplanar waveguide (CPW) technology, with capabilities up to 30 GHz, thus covering, for instance, the 3.1-10.7 GHz band as well as that for vehicular radar between 20 GHz and 29 GHz. Their geometries are similar to known 3-10 GHz UWB antennas but their frequency range has been significantly increased.

II. Design

A relatively large number of published printed-circuit UWB antennas consists of a microstrip-line-fed metalized and arbitrarily shaped patch over a removed ground plane. Our design procedure starts with a hexagon whose corner points are located on a circle. Using a time-domain technique (CST Microwave Studio) and feeding an UWB pulse to the input of the microstrip (or CPW) line, the reflected wave is Fourier transformed and the reflection coefficient monitored over a wide frequency range. For a given substrate, i.e., RT/Duroid 6002 with ε_r=2.94 and 0.762mm (30 mil) thickness, and characteristic impedance of 50 Ω of the feeding transmission line, the corners of the hexagon and angle of the ground plane are varied until the reflection coefficient is better than 10 dB over the frequency range in question.

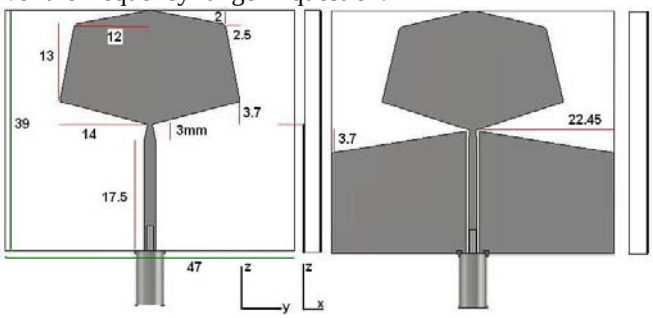

(a) (b)

Fig. 1 Schematic views and coordinate system of printed-circuit UWB antennas in microstrip (a) and CPW (b) technologies. Units are in millimetres.

Fig.1 shows the configurations and dimensional parameters of the UWB antenna structures in microstrip and CPW technologies. The gaps between the centre conductor and the ground planes in CPW technology (Fig. 1b) is selected as 0.2 mm for manufacturing purposes. In addition, the input coaxial feed line has inner and outer diameters of 1 mm and 3.3 mm, respectively, separated by Teflon material. Note that the

978-1-4577-1559-4/12/$26.00 ©2012 IEEE

coaxial cable is included in all simulations as it presents, first, a non-negligible reflection at its interface to the printed-circuit board and, secondly, connects the two ground planes in the CPW design (Fig. 1b).

III. Results

Fig. 2 shows the reflection coefficients of both the microstrip and CPW antennas. Between 2.8 GHz and 30 GHz, $|S_{11}|$ is less than -10dB, thus validating the design procedure to obtain a broadband match.

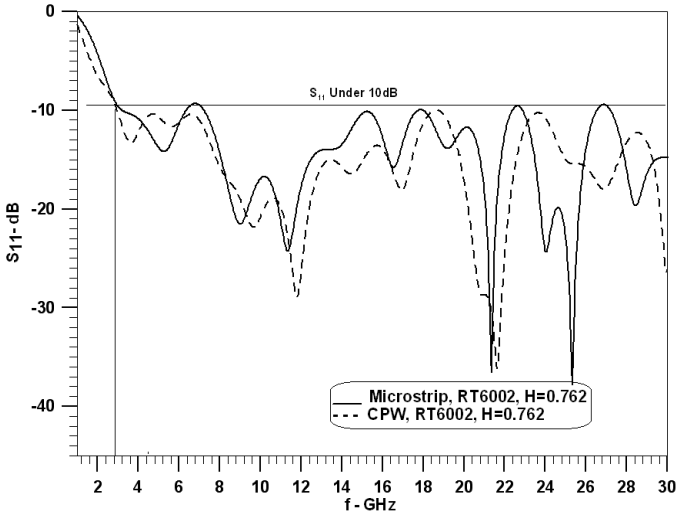

Fig. 2 Reflection coefficients in dB of the microstrip (solid line) and CPW (dashed line) UWB antennas. Units are in millimetres.

In order to compute the amplitude and phase responses, a probe is located in the far field of the antenna. The pulse fed to the input of the antenna and that received by the probe are Fourier transformed and their amplitude and phase relation ship extracted. The phase information is usually presented as group delay, the derivative of the phase response with respect to angular frequency. The results are presented here only for a single preferred direction as the analysis over an entire sphere requires modelling of a large structure (due to low-frequency far-field conditions) or establishing multi-scale dimensions.

Fig. 3 shows the amplitude and group delay plots over the entire frequency range. The probe is located at θ=90 and ϕ=90 degrees which is the right horizontal direction in Fig. 1. The low amplitude level in Fig. 3a is due to the extremely small size of the probe and its omnidirectional characteristic. While the vertical polarization E_θ of both antennas is reasonably constant over the entire frequency range, the horizontal (cross) polarization E_ϕ increases with frequency and, between 26 GHz and 28 GHz, shows levels in the same order of magnitude for the microstrip antenna. This would permit the use of dual-polarized applications if required, especially since also the group delay (Fig. 3b) is almost identical in this narrow frequency range. Note that the cross polarization of the microstrip antenna is usually higher because this polarization is present in the microstrip feed but absent from that of the CPW.

In general, the group delay performance is much flatter for vertical than horizontal polarization. The variations are 250ps and 700ps, respectively, for the microstrip antenna (Fig. 3b) and 180ps and 950ps, respectively, for the CPW antenna (Fig. 3c). This performance is comparable to many other printed-circuit UWB antennas, albeit their group delay responses are confined to a much smaller frequency range - the regular 3-10 GHz region.

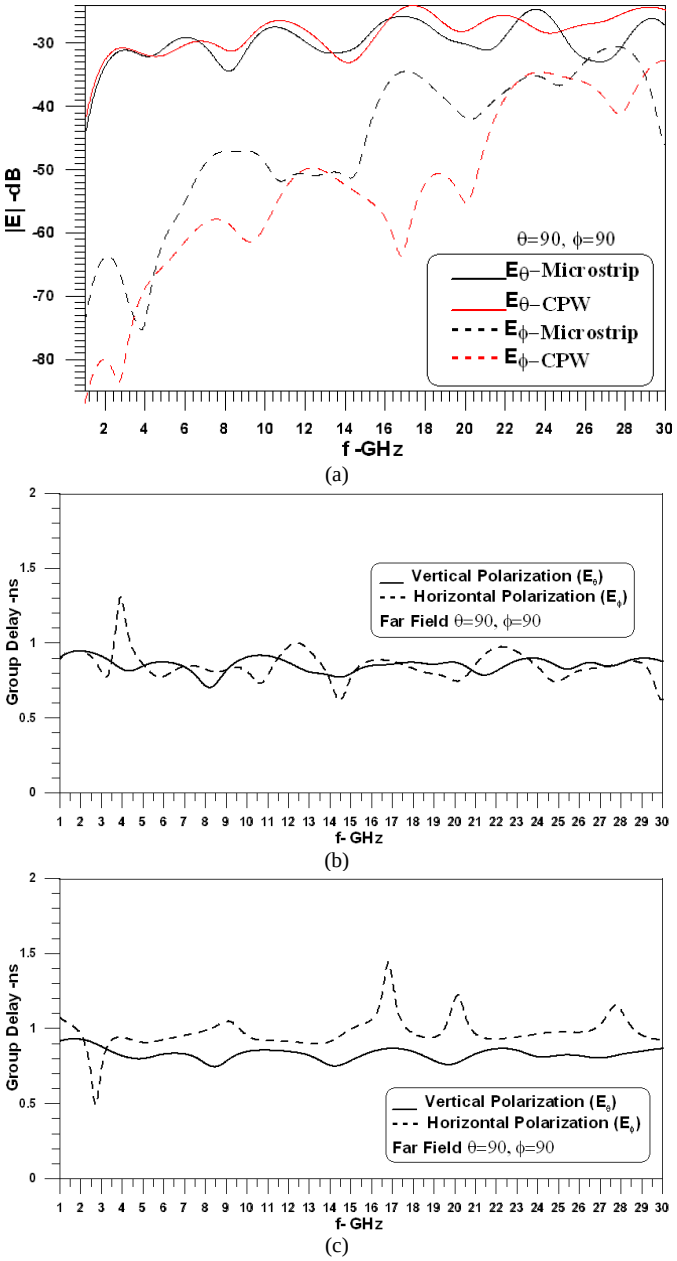

Fig. 3 Responses of microstrip and CPW UWB antennas; amplitude responses (a), and group delay of the microstrip (b) and CPW (c) antennas.

Fig. 4 shows the E-plane radiation characteristics of the microstrip antenna for 14 different frequencies. It is obvious that in the lower frequency range, the antenna behaves like a typical monopole whereas towards higher frequencies, the number of minima increases due to the reducing wavelength. A similar observation can be made for the CPW antenna (Fig. 5). It is important to note, though, that radiation in the θ=±90 degree directions is always present for both antennas. H-plane

radiation patterns are omitted here for lack of space. Their characteristics are close to omnidirectional in the lower frequency range but show an increasing number of minima in the upper and lower direction (c.f. Fig. 1) as the frequency increases. Thus the characteristics change to a more directional pattern with progressing frequency.

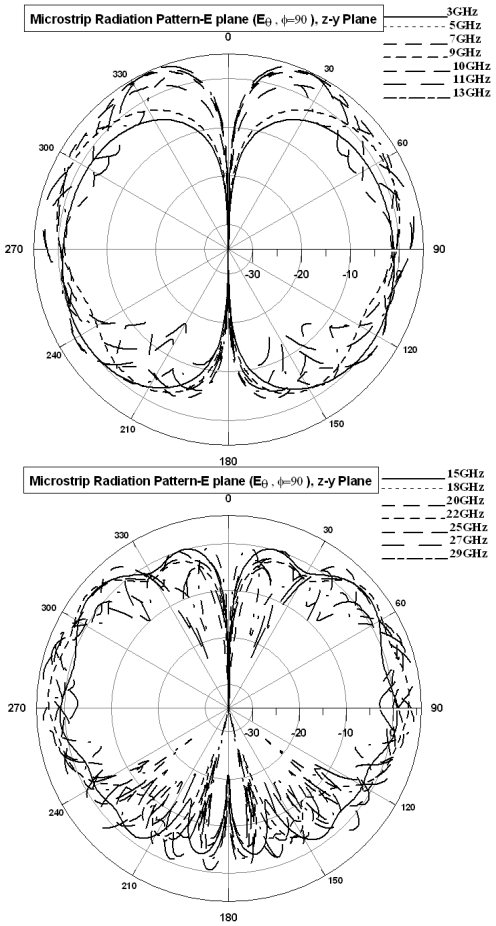

Fig. 4 E-plane radiation patterns of the microstrip UWB antenna.

It is difficult to present gain plots for a UWB antenna as the direction of the main beam changes with frequency. Therefore, we adopted two approaches. The first one shows the vertically polarized gains in specific planes. In Fig. 6 we plot the maximum E-plane gain obtained at varying angles θ in the E-plane at ϕ=90 degrees, i.e., the *yz* plane in Fig. 1. The H-plane gain is the maximum gain at varying angles ϕ at θ=90 degrees, i.e., the *xy* plane. Both microstrip and CPW antennas in Fig. 6a and Fig. 6b, respectively, show variations typical of UWB antennas, and the average gain increases with frequency. Note that gain values below 0 dB in the lower frequency range indicate that the direction of maximum gain might have shifted to a direction different from angles in the E- or H-planes.

The second approach consists in presenting the vertically polarized gain in a preferred direction and is termed 'realized gain'. The related data is shown in Fig. 7 for the θ=ϕ=90 degree direction. This gain varies rapidly for both antennas but shows better results for the CPW antenna. Note that a dip

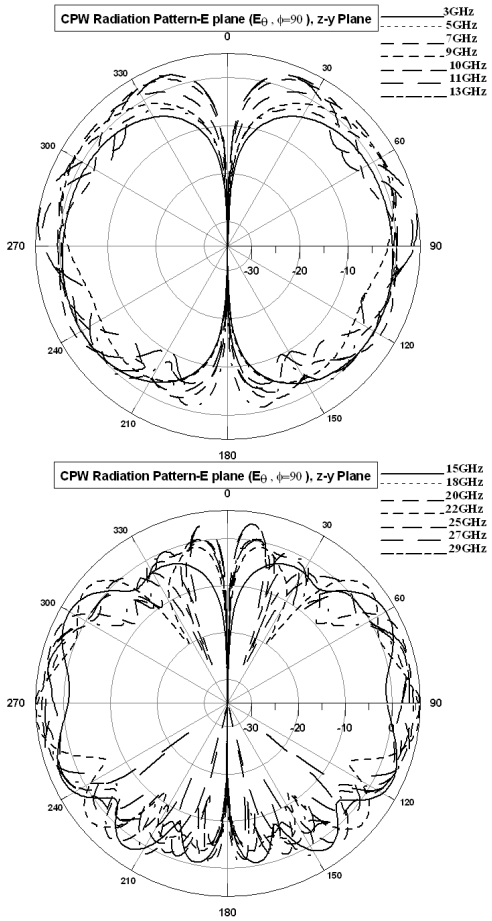

Fig. 5 E-plane radiation patterns of the CPW UWB antenna.

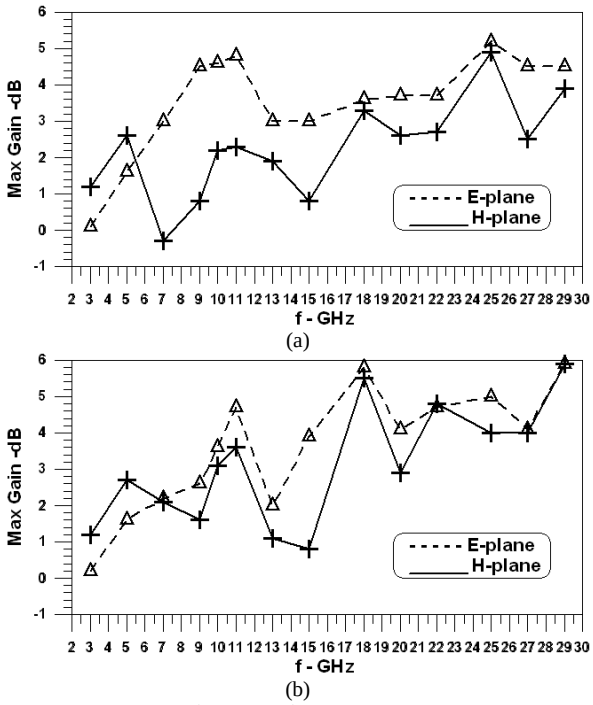

Fig. 6 Maximum gain performances for microstrip (a) and CPW (b) antennas as the probe moves along the E- and H planes.

occurs for the microstrip antenna in Fig. 7 (at 27 GHz) which is the same frequency where previously a dual-polarization operation was envisaged. It is thus obvious that the microstrip antenna's co-polarized (vertically polarized) gain drops as half of the power is already radiated in the cross-polar (horizontal) direction. For remote monitoring or surveillance purposes, though, it is vital that the antenna receives a signal. Its actual strength is of secondary importance.

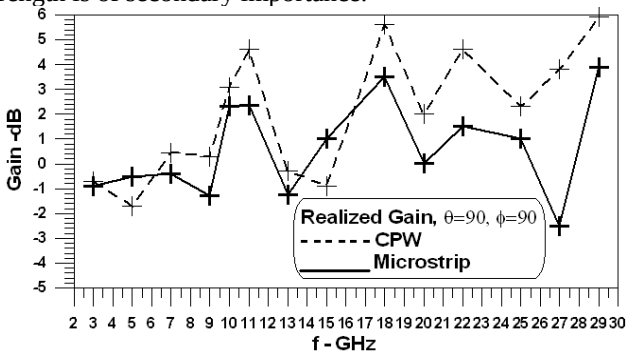

Fig. 7 Realized gain performances of the main electric field (E_θ) for both antennas, while the probe is located at θ=90 and ϕ=90.

IV. Conclusions

The two new printed-circuit antennas for ultra-wideband (UWB) monitoring applications are shown to operate between 3 GHz and 30 GHz with a return loss of 10 dB. Their amplitude and group delay performances are acceptable and compare well with other UWB printed-circuit antennas which have previously been presented for only the 3-10 GHz frequency range. The gain of both antennas, however, varies drastically in specific directions and/or planes, since the main beam or multiple main beams change directions with frequency. It is thus expected that such antennas be mobile when employed in monitoring or surveillance equipment. The microstrip antenna shows possibility of dual-polarized applications in the higher frequency range, but the coplanar antenna demonstrates slightly better amplitude, group delay and gain performance overall.

Acknowledgment

The authors wish to acknowledge support for this work from the Natural Sciences and Engineering Research Council of Canada and the TELUS Research Grant in Wireless Communications.

References

[1] A.L. Amadjikpè, D. Choudhury, G.E. Ponchak, and J. Papapolymerou, "Location specific coverage with wireless platform integrated 60-GHz antenna systems," *IEEE Trans. Antennas Propagat*., vol. 59, pp. 2661-2671, July 2011.

[2] J.D. Brunett, R.M. Ringler, and V.V. Liepa, "On measurements for EIRP compliance of UWB devices," *IEEE EMC-S Int. Symp. Dig.*, pp. 473-476, Chicago, USA, Aug. 2005.

[3] C. Yoon, H. Park, W. Lee, M. Shin, J.S. Pak, and J. Kim, "Power/ground noise immunity test in wireless and high-speed UWB communication system," *IEEE EMC-S Int. Symp. Dig.*, pp. 1-6, Detroit, USA, Aug. 2008.

[4] H. Kamiya, M. Yamada, M. Tokuda, S. Ishigami, K. Gotoh, and Y. Matsumoto, "A new method for measuring interference between UWB and wireless LAN systems," *Proc. Int. Wireless Communications and Mobile Computing Conference*, pp. 1106-1111, Crete, Greece, Aug. 2008.

[5] C. Adami, C. Braun, P. Clemens, M. Suhrke, H.U. Schmidt, and A. Taenzer, "HPM detection system for mobile and stationary use," *Proc. Int. Symp. Electromagnetic Compatibility*, pp. 1-6, York, UK, Sep. 2011.

[6] O. Lauer, M. Riederer, N. Karoui, R. Vahldieck, E. Keller, and J. Fröhlich, "Characterization of the electromagnetic environment in a hospital," *Proc. Asia-Pacific Symp. Electromagnetic Compatibility*, pp. 474-477, Singapore, May 2008.

[7] M. Barbiroli, C. Carciofi, and D. Guiducci, "Assessment of population and occupational exposure to Wi-Fi systems: Measurements and simulations," *IEEE Trans. Electromag. Compat.*, vol. 53, pp. 219-228, Feb. 2011.

[8] J. Zhang, P.V. Orlik, Z. Sahinoglu, A.F. Molisch, and P. Kinney, "UWB systems for wireless sensor networks," *Proc. IEEE*, vol. 97, pp. 313-331, Feb. 2009.

[9] J. Yu, Y. Cen, S. Chen, S. Wai, X. Chen, S. Liu, M. Zhou, and Y. Gaol, "Design of EMC testing equipment for mobile phones," *Proc. Int. Conf. Microwave Technology and Computational Electromagnetics*, pp. 192 – 195, Beijing, China, Nov. 2009.

[10] C. Hoffmann and P. Russer, "A broadband high-dynamic time-domain system for EMI measurements in K-band up to 26 GHz," *IEEE EMC-S Int. Symp. Dig.*, pp. 489-492, Long Beach, USA, Aug. 2011.

[11] K. Chung, S. Pyun and J. Choi, "Design of an ultrawide-band TEM horn antenna with a microstrip-type balun", *IEEE Trans. Antennas Propogat*., vol. 53, pp. 3410-3413, Oct. 2005.

[12] E.S. Pires, P.I.L. Ferreira, G. Fontgalland, M.A.B. de Melo, R.M. Valle, and T.P. Vuong, "Design of a UWB antenna for sensor and wireless systems applications," *Proc. IEEE Int. Conf. Ultra-Wideband*, pp. 185-188, Hannover, Germany, Sep. 2008.

[13] H.-J. Lam and J. Bornemann, "Ultra-wideband printed-circuit antenna in coplanar technology," *IEEE EMC-S Int. Symp. Dig*., TU-PM-1-7, pp. 1-4, Honolulu, USA, July 2007.

[14] M.A. Peyrot-Solis, G.M. Galvan-Tejada, and H. Jardon-Aguilar, "Directional UWB planar antenna for operation in the 5-20 GHz band," *Proc. 17th Int. Zurich Symp. EMC*, pp. 277-280, Singapore, Feb./Mar. 2006.

[15] J. Liu, K.P. Esselle, and S. Zhong, "Creating multiple band notches in an extremely wideband printed monopole antenna," *Proc. Asia-Pacific Microwave Conf.*, pp. 2220-2223, Yokohama, Japan, Dec. 2010.

[16] K. Rambabu, H.A. Thiart, J. Bornemann and S.Y. Yu, "Ultrawideband printed-circuit antenna", *IEEE Trans. Antennas Propagat.*, vol. 54, pp. 3908-3911, Dec. 2006.

[17] J. Bai, S. Shi, and D.W. Prather, "Modified compact antipodal Vivaldi antenna for 4–50-GHz UWB application," *IEEE Trans. Microwave Theory Tech.*, vol. 59, pp. 1051-1057, Apr. 2011.

[18] M. Mokhtaari and J. Bornemann, "Printed-circuit antennas for 3-30 GHz and 3-60 GHz UWB applications," *Proc. Asia-Pacific Microwave Conf.*, pp. 1922-1925, Yokohama, Japan, Dec. 2010.